



1 **Sensitivity of modeled Indian Monsoon to Chinese and Indian aerosol**  
2 **emissions**

3 Peter Sherman<sup>1</sup>, Meng Gao<sup>2,3</sup>, Shaojie Song<sup>3</sup>, Alex T. Archibald<sup>4,5</sup>, Nathan Luke Abraham<sup>4,5</sup>,  
4 Jean-François Lamarque<sup>6</sup>, Drew Shindell<sup>7</sup>, Gregory Faluvegi<sup>8,9</sup>, Michael B. McElroy<sup>1,3</sup>

5 <sup>1</sup>Department of Earth and Planetary Sciences, Harvard University, Cambridge, Massachusetts,  
6 United States

7 <sup>2</sup>Department of Geography, Hong Kong Baptist University, Hong Kong SAR, China

8 <sup>3</sup>School of Engineering and Applied Sciences, Harvard University, Cambridge, Massachusetts,  
9 United States

10 <sup>4</sup>National Centre for Atmospheric Science, University of Cambridge, Cambridge, UK

11 <sup>5</sup>Department of Chemistry, University of Cambridge, Cambridge, UK

12 <sup>6</sup>National Center for Atmospheric Research, Boulder, Colorado, USA

13 <sup>7</sup>Nicholas School of the Environment, Duke University, Durham, NC, USA

14 <sup>8</sup>NASA Goddard Institute for Space Studies, New York, NY

15 <sup>9</sup>Center for Climate Systems Research, Earth Institute, Columbia University, New York NY

16



17 **Abstract**

18 The South Asian summer monsoon supplies over 80% of India's precipitation. Industrialization  
19 over the past few decades has resulted in severe aerosol pollution in India. Understanding  
20 monsoonal sensitivity to aerosol emissions in general circulation models (GCMs) could improve  
21 predictability of observed future precipitation changes. The aims here are (1) to assess the role of  
22 aerosols on India's monsoon precipitation and (2) to determine the roles of local and regional  
23 emissions. For (1), we study the Precipitation Driver Response Model Intercomparison Project  
24 experiments. We find that the precipitation response to changes in black carbon is highly uncertain  
25 with a large intermodel spread due in part to model differences in simulating changes in cloud  
26 vertical profiles. Effects from sulfate are clearer; increased sulfate reduces Indian precipitation, a  
27 consistency through all of the models studied here. For (2), we study bespoke simulations, with  
28 reduced Chinese and/or Indian emissions in three GCMs. A significant increase in precipitation  
29 (up to ~20%) is found only when both countries' sulfur emissions are regulated, which has been  
30 driven in large part by dynamic shifts in the location of convective regions in India. These changes  
31 have the potential to restore a portion of the precipitation losses induced by sulfate forcing over  
32 the last few decades.

33



#### 34 **Significance Statement**

35 The aims here are to assess the role of aerosols on India's monsoon precipitation and to determine  
36 the relative contributions from Chinese and Indian emissions using CMIP6 models. We find that  
37 increased sulfur emissions reduce precipitation, which is primarily dynamically driven due to  
38 spatial shifts in convection over the region. A significant increase in precipitation (up to ~20%) is  
39 found only when both Indian and Chinese sulfate emissions are regulated.

40



## 41 **1. Introduction**

42 The South Asian summer monsoon is the dominant weather pattern over India, lasting typically  
43 from June to September. Over this period, southwesterly winds transport warm, moist air from the  
44 Arabian Sea onto the Indian subcontinent, supplying roughly 80% of the region's annual rainfall  
45 (Turner and Annamalai, 2012). Since the monsoon provides such a significant source for India's  
46 water supply, changes in its strength and position would have important socioeconomic  
47 implications including though not simply confined to agricultural production (Kumar et al., 2004;  
48 Douglas et al., 2009) and drought frequency (Subbiah, 2002). Given the rugged orography of the  
49 surrounding region and difficulties in modelling intense precipitation, resolving the future roles of  
50 natural variability and the externally forced signal for the monsoon is a fundamentally difficult –  
51 but important – problem.

52

53 Interannual changes in the monsoon have been linked to internal (natural) variability inherent to  
54 the climate system. For instance, numerous studies have found a potential connection between  
55 variability in the El Niño-Southern Oscillation (ENSO) and the monsoon (Sikka 1980; Shukla and  
56 Paolino 1983; Annamalai and Liu 2005). Such links could be used to improve predictability of  
57 Indian rainfall. While internal variability likely plays a non-negligible role in modulating the South  
58 Asian summer monsoon – and is expected to continue to do so in the future, even in high emissions  
59 scenarios (Annamalai et al. 2007) – changes in the monsoon's mean state associated with external  
60 forcings are also of fundamental importance. Specifically, determining the anthropogenic impacts  
61 on monsoonal changes associated with emissions of greenhouse gases (GHGs) and aerosols can  
62 provide critical insights that can help better inform policymaking decisions regarding emission  
63 regulations.



64

65 The steady rise in GHGs over the 20<sup>th</sup> century has increased the atmosphere's average temperature  
66 and water vapor content through the Clausius-Clapeyron relation, and might be expected as a result  
67 to contribute to increased precipitation over India. CMIP6 models run with just an increase in CO<sub>2</sub>  
68 forcing exhibits such an increase uniformly across India (Figure S1). However, in reality the  
69 picture is more complex as the literature has indicated no such observed trend for India over the  
70 last half century (Ramesh and Goswami, 2014; Saha and Ghosh, 2019). Observed monsoon  
71 precipitation aggregated over all of continental India (Figure 1) actually indicates a slight drying  
72 trend over the last few decades. While these trends are not statistically significant at a 95%  
73 confidence level, the purpose of Figure 1 is to illustrate that the increase in monsoon precipitation  
74 expected from the growing greenhouse forcing has certainly not been detected. There may be  
75 several mechanisms invoked to explain why Indian monsoon precipitation has not increased. Land  
76 use changes over the Indo-Gangetic Plain have been implicated as one of the causes, where  
77 decreased evapotranspiration may have limited the amount of available precipitable water in the  
78 region (Paul et al., 2016). It has been shown also that aerosol effects have counterbalanced the  
79 precipitation changes attributable to the greenhouse warming (Bollasina et al., 2011; Turner and  
80 Annamalai, 2012). Ramanathan et al. (2005) found that aerosols over India reduce surface  
81 shortwave radiation, which limits the amount of evaporation and thereby reduces monsoon  
82 precipitation. Additionally, it has been shown that the atmospheric brown cloud (originally so  
83 termed in Ramanathan and Crutzen, 2003, referring to the pervasive light absorbing aerosol layer  
84 akin to the stratocumulus cloud decks observed over the oceans) over the Northern Indian Ocean  
85 is associated with a stable atmosphere that limits convection. Atmospheric brown clouds consist  
86 primarily of black and organic carbon, dust and other anthropogenic aerosols. Sources of aerosols



87 and their precursors in South and East Asia (indicated in Figure S2), are tied particularly to energy  
88 production and biomass combustion, which have grown steadily in response to industrialization in  
89 the region, though recent trends in these two regions differ. Meehl et al. (2008) similarly found  
90 that an increased aerosol load reduced precipitation over India during the monsoon season, but that  
91 it also increased rainfall in the pre-monsoon season. Wang et al. (2009) found that absorbing  
92 aerosols were particularly important in influencing the summer monsoon system. The issue with  
93 many of these studies is that they focus on individual models. There is a large spread in the  
94 precipitation response across models reflecting differing representations of cloud and aerosol  
95 processes (e.g. Wilcox et al., 2015), factors that may bias results given the already complex nature  
96 of modelling precipitation over India (Ramanathan et al., 2005; Bollasina et al., 2011; Turner and  
97 Annamalai, 2012; Ramesh and Goswami, 2014; Paul et al., 2016; Saha and Ghosh, 2019).  
98 Multimodel ensembles can improve our understanding and help constrain uncertainty on the  
99 impacts of different aerosol constituents on the monsoon.

100

101 Here, we analyze results from two climate model intercomparisons to better understand the  
102 summer monsoonal impacts from sulfur and black carbon aerosols, two of the dominant  
103 constituents of India's aerosol pollution. First, we study the Precipitation Driver Response Model  
104 Intercomparison Project (PDRMIP; Samset et al. 2016) experiments to assess the summer  
105 monsoon response to extreme aerosol conditions. The purpose of the PDRIMP experiments is to  
106 determine if a precipitation signal can be detected i.e. a causal link between the emissions of sulfur  
107 and black carbon and changes in the monsoon. Previous analysis of a set of PDRMIP experiments  
108 which increase global BC levels tenfold found a slight enhancement in P-E during the South Asian  
109 summer monsoon, driven by a strengthened land-sea temperature gradient (Xie et al., 2020). We



110 focus the first section of our analysis on Asian perturbation experiments as significant emissions  
111 changes are expected over this region in the coming decades (e.g. Samset et al., 2019). We note  
112 that these experiments use artificially large emission perturbations to enable isolation of signal  
113 detection from climatic variability. Second, we study a set of regional aerosol emissions  
114 intercomparison experiments (labeled RAEI experiments for the rest of the paper for convenience)  
115 to assess the relative contributions of Indian and Chinese anthropogenic aerosol emissions to the  
116 monsoon. Because remote emissions may play an important role on India's monsoon (e.g. Shawki  
117 et al. 2018), in addition to Indian emissions we choose to study emissions from China because this  
118 country is presently the world leading emitter of BC and SO<sub>2</sub>, is in close proximity to India and its  
119 emissions of both pollutants are expected to decline rapidly over the coming decade. Emissions in  
120 more remote regions are less likely to change in a major way. A robust analysis of these  
121 intercomparisons should refine our understanding of the anthropogenic influence on the South  
122 Asian summer monsoon and reduce uncertainty on future changes given that India's anthropogenic  
123 emissions are expected to increase at least in the near term, while China's will likely decrease (Rao  
124 et al. 2016). We decompose precipitation changes into dynamic (i.e. circulation changes) and  
125 thermodynamic (i.e. specific humidity changes) components to assess how aerosols interact with  
126 the monsoon. The rest of the paper is structured as follows: section 2 discusses the simulations  
127 used in the analysis, section 3 presents and analyzes potential monsoonal impacts associated with  
128 sulfur and black carbon emissions and section 4 summarizes the study and highlights needs for  
129 future work.

130

## 131 **2. Data and Methods**

### 132 *2.1 PDRMIP intercomparison*



133 We first study the Precipitation Driver Response Model Intercomparison Project (PDRMIP)  
134 experiments. PDRMIP is an idealized set of modelling experiments, used to better understand  
135 drivers of regional precipitation change. We focus specifically on two experiments that involve  
136 perturbations to Asian concentrations or emissions (see Table 1), where Asia is defined by the  
137 regional box of 60-140°E and 10-50°N. The first is BC10xASIA, representing a tenfold increase  
138 in present-day BC concentrations or emissions in Asia at all vertical levels, and the second is  
139 SULF10xASIA, which explores a similar tenfold increase in present-day sulfate concentrations or  
140 emissions. The BC10xASIA and SULF10xASIA scenarios are compared with control simulations  
141 (henceforth called CTRL<sub>PDRMIP</sub>) where aerosol concentrations or emissions are maintained at near  
142 current values (either year 2000 or 2005 for each model). We study the six models involved in the  
143 PDRMIP experiments that conduct the Asian perturbation experiments (Table 1). These  
144 experiments will be used to better constrain uncertainty on the direction of precipitation and  
145 circulation changes under anthropogenic aerosol emissions changes. Since these are extreme  
146 perturbations to aerosol concentrations, we use these scenarios not as representative of a future  
147 emissions trajectory, but rather as a way to check if different models with different process  
148 representations indicate a consistent response. Due to inter-model differences in spatial resolution,  
149 all data are rescaled to the lowest model resolution ( $3.75^\circ \times 2.0^\circ$ ) when comparing model output.  
150 Variations in aerosol schemes and direct and indirect aerosol effects across the six models will  
151 affect the spread in predicted precipitation changes associated with the increased aerosol  
152 concentrations (Table 1). The different schemes and their effects on precipitation will be discussed  
153 further in the section 3.

154



155 **Table 1.** Details of the models analyzed in this work. For the models participating in the  
 156 PDRMIP Asian aerosol perturbation simulations, each simulation lasts 100 years. Cloud scheme  
 157 refers to the microphysical cloud scheme that describes cloud formation, where a one-moment  
 158 scheme considers only changes in mass and a two-moment scheme considers changes in mass  
 159 and number concentration. The first indirect effect refers to the aerosol effect on cloud albedo  
 160 and the second indirect effect refers to the aerosol effect on cloud lifetime.

Model	Spatial resolution	Cloud scheme	Indirect effects	Model reference	Aerosol microphysics	MIP
CESM1-CAM5 <sup>†</sup>	1.25° × 0.9375°	Two moment	First, second	Neale et al. (2012)	Full aerosol	PDRMIP, RAEI
GISS-E2-R	2.5° × 2.0°	One moment	None*	Schmidt et al. (2014)	No aerosol	PDRMIP, RAEI
HadGEM3	1.875° × 1.25°	One moment	First	Hewitt et al. (2011)	No BC; aerosol-cloud interaction included	PDRMIP
UKESM1-0-LL	1.875° × 1.25°	Two moment	First, second	Sellar et al. (2019)	Full aerosol	RAEI
IPSL-CM	3.75° × 1.875°	Two moment	First, second	Dufresne et al. (2013)	Aerosol microphysics for Twomey effect	PDRMIP
NorESM	2.5° × 1.875°	Two moment	First, second	Bentsen et al. (2013)	Full aerosol	PDRMIP
MIROC-SPRINTARS <sup>†</sup>	1.41° × 1.41°	One moment	First, second	Watanabe et al. (2011)	Full aerosol	PDRMIP

161 \*Indirect effects in the PDRMIP simulations were turned off since these simulations had prescribed aerosol fields  
 162 and so changes in the hydrologic cycle could not change the aerosols. The first effect was included in the GISS RAEI  
 163 simulations, however, as those are emissions-driven and hence physically consistent.

164 †Indicate models that change emissions in the PDRMIP experiments. Rows that do not include this mark indicate  
 165 models that change concentrations in the PDRMIP experiments.

## 166 2.2 RAEI experiments

168 The purpose of the RAEI experiments is to assess the relative contributions of aerosol emissions  
 169 from China and India on monsoon precipitation over India. Three GCMs with coupled chemistry-  
 170 climate components are used to study the effects of regional perturbations in aerosol emissions on  
 171 the Indian monsoon: GISS-E2-R (Schmidt et al., 2014), CESM1-CAM5 (Neale et al., 2012) and  
 172 UKESM1-0-LL (Sellar et al., 2019). Past research has used some of these models to explore the



173 effects of regional aerosol reductions on global precipitation, including emissions changes in the  
174 US, Europe, China and India. Some of the experiments from RAEI have been used to study the  
175 global effects of US SO<sub>2</sub> emissions on global precipitation (Conley et al., 2018) as well as local  
176 and remote precipitation responses to regional reductions in aerosols (Westervelt et al., 2018).  
177 Here, we study the South Asian summer monsoon response to reductions in anthropogenic aerosol  
178 emissions in China and India, focusing specifically on a set of three experiments: (1) no SO<sub>2</sub>  
179 emissions in India (IND NO SO<sub>2</sub>), (2) 80% SO<sub>2</sub> emissions reduction in China (CHN 20% SO<sub>2</sub>)  
180 and (3) no SO<sub>2</sub> emissions in India and China (IND+CHN NO SO<sub>2</sub>). We have run additional BC  
181 experiments that are included only in the SI because we find that changes in BC do not have a  
182 clear impact on precipitation in the summer monsoon. The three SO<sub>2</sub> experiments will be compared  
183 to control simulations (CTRL) with emissions set near present-day values (year 2000 or 2005  
184 depending on the model) to determine the relative importance on summer monsoon precipitation  
185 of regional aerosol emissions from India and China. The UKESM experiments were run over a  
186 shorter period (40 years), relative to the other models (~200 years). We found from resampling  
187 that 40 years is sufficient to observe the general precipitation statistics over India. For  
188 climatological variables studied in our PDRMIP and RAEI analysis, we take mean values over the  
189 full simulation period, excluding the first 10 years to allow for spin-up.

190

### 191 *2.3 Precipitation decomposition*

192 In addition to calculating overall precipitation changes due to sulfur and BC emissions, we seek  
193 also to determine the dynamic and thermodynamic components of the changes attributable to these  
194 forcing agents. The dynamic component is representative of precipitation changes caused by a  
195 change in atmospheric circulation, and the thermodynamic component is representative of



196 variations in precipitation due to changes in moisture under constant circulation. To perform this  
197 decomposition, we follow the methodology of Chadwick et al. 2016. The total precipitation change  
198  $\Delta P$  can be expressed as

$$199 \quad \Delta P = \Delta q M^* + q \Delta M^* + \Delta q \Delta M^*,$$

200 where  $q$  is the near-surface specific humidity and  $M^*$  is a proxy for convective mass flux ( $M^* =$   
201  $P/q$ ). The first term on the right hand side is representative of thermodynamic changes ( $\Delta P_{\text{therm}}$ ),  
202 the second dynamic changes ( $\Delta P_{\text{dyn}}$ ) and the third the nonlinear interaction of these two  
203 components ( $\Delta P_{\text{cross}}$ ).  $\Delta P_{\text{dyn}}$  can be further decomposed into shifts in the circulation patterns  
204 ( $\Delta P_{\text{shift}}$ ) and changes in the mean strength of the tropical circulation ( $\Delta P_{\text{strength}}$ ) as

$$205 \quad \Delta P_{\text{shift}} = q \Delta M^*_{\text{shift}},$$

$$206 \quad \Delta P_{\text{strength}} = q \Delta M^*_{\text{strength}},$$

207 where  $\Delta M^*_{\text{strength}} = -\alpha M^*_{\text{strength}}$  (where  $\alpha = \text{tropical mean } \Delta M^* / \text{tropical mean } M^*$ ).  $\Delta M^*_{\text{shift}}$  is  
208 computed as the residual of  $\Delta M^*$  and  $\Delta M^*_{\text{strength}}$ . This decomposition follows the methodology in  
209 Chadwick et al. 2016 and Monerie et al. 2019.

210

### 211 **3. Results**

#### 212 *3.1 PDRMIP analysis: summertime Indian precipitation response to large BC and sulfur* 213 *perturbations*

214 We start with an evaluation using the PDRMIP experiments (Table 1) of summertime Indian  
215 precipitation changes caused by large BC and sulfate concentration increases over all of Asia. The  
216 difference in summer precipitation between the BC10xASIA and CTRL<sub>PDRMIP</sub> experiments  
217 provides an estimate for the role of BC in monsoonal changes and is shown in Figures 2a-g. From  
218 the individual models (Figures 2a-f), there is a noticeably large ensemble spread in the



219 precipitation response over India due to the increase in BC. In north India, for example, HadGEM3  
220 shows a precipitation decrease of up to 70%, while SPRINTARS exhibits effectively a null  
221 response and GISS is identified with a strong precipitation increase of ~50%. PDRMIP simulations  
222 that globally increase BC tenfold also do not show a consistent multimodel response over India  
223 (Samset et al. 2016; Liu et al 2018). While HadGEM3 and GISS generally underestimate  
224 precipitation over India (Figure S3), it does not appear that these biases are manifest in consistent  
225 precipitation changes in the BC10xASIA experiments. Additionally, while two of the six models  
226 studied increase BC emissions rather than BC concentrations, this does not appear to alter the BC  
227 vertical profile except in the stratosphere (see Figure S4). It is likely that different aerosol schemes  
228 across models (Table 1) may be implicated as the dominant source of the large ensemble spread,  
229 although both the boundary layer scheme and modelling impacts of absorbing aerosols on cloud  
230 formation (Koch and Del Genio, 2010) could play important roles. Specifically, cloud formation  
231 is affected significantly by the BC vertical profile; BC within the cloud layer can burn off moisture  
232 and reduce cloud cover, BC below the cloud layer can enhance convection and increase cloud  
233 cover and BC above the cloud layer can either increase or decrease cloud cover according to the  
234 cloud type. Because of the complexities of the semi-direct effects of absorbing aerosols that are  
235 currently not heavily constrained by observations, the role of BC generally has a diverse response  
236 across climate models (Koch et al., 2009; Stjern et al. 2017). Large variance in the cloud fraction  
237 vertical profile are apparent also in the PDRMIP BC10xASIA simulations (Figure 3). This large  
238 uncertainty does not consistently favor an increase or decrease in cloud fraction across vertical  
239 layers except in NorESM and CESM where a slight increase (on the order of a couple of percent)  
240 can be detected across all layers. Variations in the BC vertical profile as well as its lifetime can  
241 result in significant changes in cloud cover and precipitation even within an individual model by



242 changing atmospheric stability and humidity (Samset and Myhre 2015). These effects are manifest  
243 in the diverse shortwave responses (Figure S5), which indicate a large spread between models in  
244 magnitude and sign over parts of India. Additionally, changes in the TOA net radiative forcing  
245 between BC10xASIA and PDRMIP<sub>CTRL</sub> are generally consistent in magnitude and direction across  
246 models over India (Figures S7a-f). By contrast, the change in Cloud Radiative Effect (CRE;  
247 Figures S7g-l) is not consistent in sign across models, suggesting that the models agree on the  
248 direct aerosol effects but differ on the aerosol-cloud interactions. While there are more causative  
249 factors on precipitation than cloud fraction, the important point is that because of the large cloud  
250 uncertainty that varies in both magnitude and sign, it is difficult to attribute future changes in  
251 Indian precipitation to changes in BC concentration. This is reflected in the precipitation change  
252 which fails to demonstrate a clear spatial coherence in the multimodel mean (Figure 2g).

253

254 The role of sulfate for Indian precipitation is much clearer. The percent change in precipitation  
255 between the SULF10xASIA and CTRL PDRMIP experiments is shown in Figures 2h-n. The sign  
256 of the precipitation change is generally consistent across models, with a large decrease in  
257 precipitation (~50%) over all of India in response to a tenfold increase in sulfate. There is also  
258 large uncertainty in the cloud fraction profile response to sulfate emissions (Figure 3), similar to  
259 the BC PDRMIP experiments. However, five of the six models on average favor a decrease in  
260 cloud fraction with increased SO<sub>2</sub> emissions, consistent with the precipitation response. So, while  
261 there is a comparable measure of intermodel spread for the BC10xASIA and SULF10xASIA cloud  
262 responses, the mean change is more consistent in the SULF10xASIA experiments. The results  
263 from the PDRMIP experiments, with their higher sulfate concentrations, constrain uncertainty on



264 the sign of precipitation changes, and can be used as a frame of reference for the country-specific  
265 aerosol experiments described in section 3.2 and beyond.

266

267 *3.2 RAEI analysis: Indian aerosol burden response to Chinese and Indian aerosol emissions*  
268 *changes*

269 We now consider the RAEI emissions scenarios for China and India. Percent changes in sulfate  
270 burden between the sulfate regulation scenarios and control runs are shown in Figures S7a-i. Indian  
271 sulfate emissions play an important role on local sulfate concentrations, contributing up to 60% of  
272 the country's aerosol burden, while China's emissions can contribute up to 60% over the  
273 Himalayas. The change in Indian aerosol burden for sulfate is notably consistent in terms of both  
274 the magnitude of the change as well as the spatial pattern across the three models studied. Since  
275 the temperature gradient between the Arabian Sea and Bay of Bengal and the Himalayas has been  
276 invoked as a modulator of the South Asian Monsoon (e.g. Priya et al., 2017), both Indian and  
277 Chinese emissions could influence monsoon precipitation over India by modifying the optical  
278 properties of the atmosphere not only over the country but also over surrounding regions.

279

280 *3.3 RAEI analysis: summer monsoon precipitation response to regional SO<sub>2</sub> emissions changes*

281 The precipitation response associated with SO<sub>2</sub> emissions is significant over parts of India (Figures  
282 4a-i), in agreement with the PDRMIP results. Almost all models and scenarios show an increase  
283 in summer precipitation in India when SO<sub>2</sub> emissions in China and/or India are reduced. The  
284 strongest response requires regulations from both China and India, with an increase of nearly 20%  
285 in precipitation in some regions of India when SO<sub>2</sub> emissions are reduced across the three models  
286 studied here. From these results, changes in India's precipitation depend not only on local SO<sub>2</sub>



287 emissions, but also on regional sources. These emissions can have a measurable impact on India's  
288 water availability by altering the underlying statistics in favor of greater precipitation events (e.g.  
289 Sillman et al. 2019). That being said, the spatial patterns associated with these precipitation  
290 changes vary to a large degree between models. For instance, precipitation changes in GISS exhibit  
291 greater consistency across scenarios than they do with the CESM or UKESM. Additionally,  
292 UKESM tends to estimate larger precipitation changes than the other RAEI models, consistent  
293 with the HadGEM3 results indicated in Figure 2 which uses the same physical model. There is,  
294 however, general consistency in the increase in precipitation when SO<sub>2</sub> emissions are reduced in  
295 both China and India. The precipitation responses to lower BC regional emissions are indicated in  
296 Figure S8. BC emissions play a much lesser role in GISS and CESM relative to SO<sub>2</sub> emissions,  
297 and cause an inconsistent response in UKESM across the three regional emissions experiments.  
298 For all reduced BC scenarios, the changes in India's precipitation are generally small (~5% locally)  
299 and not statistically significant at a 90% confidence level. The strongest precipitation response  
300 occurs when both Chinese and Indian BC emissions are eliminated, but there is a spread in the  
301 direction of change across models. This spread in precipitation change is consistent with that of  
302 the PDRMIP results in that the intermodel spread in precipitation change due to BC emissions  
303 changes tends to be larger than the magnitude of the precipitation response from any individual  
304 model. This may highlight large process uncertainty generally. Bond et al. (2013), for example,  
305 note that the impact of BC on the cloud radiative forcing in models is highly sensitive to the  
306 nucleation regime in the background atmosphere.

307

308 *3.4 RAEI analysis: physical understanding of the SO<sub>2</sub>-precipitation response*



309 Physical explanations for the precipitation changes induced by SO<sub>2</sub> emissions changes are  
310 explored here. Circulation changes are typically connected to sulfate increases in India; a  
311 weakened land-sea temperature gradient associated with SO<sub>2</sub> emissions would inhibit monsoonal  
312 advection of moisture from the Arabian Sea onto the Indian subcontinent. Warming over the  
313 Himalayas can be seen in most of the simulations (Figure S9), as well as changes in 850 hPa winds,  
314 where there is a clear strengthening of the coastal winds when SO<sub>2</sub> emissions are reduced (Figure  
315 4). The fact that the land-sea temperature gradient and 850 hPa winds change suggests that  
316 precipitation changes due to SO<sub>2</sub> emissions may be dynamically rather than thermodynamically  
317 driven, which motivates the precipitation decomposition analysis discussed later. As shown in  
318 Figure 4, strengthening of the monsoonal winds is largely consistent across models and scenarios,  
319 though there are slight differences in the location of the strongest zonal wind increases; in GISS  
320 and UKESM, the greatest increase is over India itself for most scenarios, while it is further south  
321 in CESM. This suggests that a high sulfate burden reduces the strength of the monsoon winds,  
322 consistent with prior studies that connect these changes to the dimming of the downward solar flux  
323 (Kim et al. 2007). The relative contributions of thermodynamic (i.e. specific humidity) changes to  
324 dynamic (i.e. circulation) changes are indicated in Figure 5. The thermodynamic precipitation  
325 response to sulfur emissions reductions is positive for the three emissions experiments, consistent  
326 with the Clausius-Clapeyron relation as less SO<sub>2</sub> increases surface temperatures and consequently  
327 specific humidity. The interaction of dynamic and thermodynamic components (panel c,  $\Delta P_{\text{cross}}$ )  
328 plays a minimal role. The magnitude of the thermodynamic response is on the order of 50% that  
329 of the dynamic component – i.e. the dynamic component dominates. Panels (d) and (e) of Figure  
330 5 indicate that this effect is driven primarily by shifts in the convective regions, with changes in  
331 the tropical mean circulation having a minimal or slightly negative effect. It is of note that the



332 magnitude of each component is consistent across the three models studied here, suggesting  
333 consistency in the mechanistic reasons for increased monsoon precipitation over India when sulfur  
334 emissions are reduced. Changing circulation patterns are suggested as a consequence of changes  
335 in CO<sub>2</sub> as well, and potential nonlinear effects of sulfur and greenhouse emissions on monsoon  
336 precipitation highlight an important point that demands further study.

337

#### 338 **4. Conclusions**

339 The main purpose of this study was to better understand, through the use of several GCM  
340 experiments, the sensitivity of the South Asian summer monsoon to regional anthropogenic aerosol  
341 emission changes. Given that this is a modelling study, there are a number of caveats that must be  
342 acknowledged. There are often questions of how well GCMs can simulate the Indian monsoon  
343 since their spatial resolution may be too coarse to resolve the complex orography of India and the  
344 surrounding regions (Prell and Kutzbach, 1992). Additionally, representation of cloud  
345 microphysical processes is a known limitation of GCMs (e.g. Wilcox et al., 2015). We find a large  
346 intermodel spread in cloud profile and precipitation changes in the various BC emissions scenarios  
347 studied here. This suggests that discrepancies in representation of cloud processes within GCMs  
348 constrain uncertainty in the precipitation response from BC perturbations, which cannot be  
349 accounted for simply by differences in the BC vertical profiles (Figure S4). In contrast, the  
350 precipitation responses for SO<sub>2</sub> emission changes as well as the dynamic mechanism for these  
351 responses are largely consistent across models, suggesting that there is relative certainty in the  
352 models ability to simulate precipitation changes due to SO<sub>2</sub> emissions. So, while it may be difficult  
353 to extrapolate on the basis of these simulations from modelled to real-world monsoon precipitation



354 changes induced by anthropogenic aerosols, consistency in the SO<sub>2</sub> response across models lends  
355 confidence in a potential observed response for future emissions changes.

356

357 On investigating the response of the monsoon to a tenfold increase of Asian BC and sulfate  
358 concentrations, we found that the role of BC on Indian precipitation is uncertain but that increased  
359 sulfate concentrations over India reduce precipitation across five of the six models studied. Large  
360 uncertainty in the precipitation response to changing Asian BC is notably consistent with previous  
361 PDRMIP analysis studying monsoon changes to a tenfold increase in global BC levels (Xie et al.  
362 2020). Consistency between the global and regional PDRMIP simulations in this context suggests  
363 further that a BC signal is difficult to detect for the South Asian summer monsoon.

364

365 When assessing the relative contributions of Chinese and Indian anthropogenic SO<sub>2</sub> emissions to  
366 aerosol loading over South Asia (the RAEI emissions experiments), and the consequent  
367 precipitation responses, we find that there is only a statistically significant difference in monsoon  
368 precipitation when there is regulation of both China and India's SO<sub>2</sub> emissions, which leads to on  
369 the order of a 20% precipitation increase locally. Consistency in the precipitation responses  
370 between the increased sulfate scenario (PDRMIP SULF10xASIA) and the decreased sulfate  
371 scenario (RAEI) suggests that the aerosol-precipitation link may be a reversible process, and is  
372 attributable in large part to dynamical changes specifically shifts in convective patterns over the  
373 region. Additionally, these results are significant because Chinese emissions of SO<sub>2</sub> have declined  
374 over the past decade, while Indian emissions have grown steadily. There is also anticipated growth  
375 in CO<sub>2</sub> emissions and concentrations over the coming decades and this is expected to result in an  
376 increase in the atmospheric water vapor content. These concurrent events will have important



377 implications for policy going forward, as water deficits present a major issue for India that may be  
378 exacerbated given the country's exponential population growth. Regions that exhibit large  
379 variability in summertime precipitation such as Chennai and Delhi (as indicated in Figure S10)  
380 may be particularly sensitive to future monsoon changes because interannual shifts between wet  
381 and dry years at present impose important strains on the available water resource. Moreover, the  
382 benefits of policies to control SO<sub>2</sub> emissions will have significant impacts not only on mitigating  
383 water deficits but also in terms of alleviation of air pollution, estimated to be responsible for  
384 hundreds of thousands of premature deaths per year in India (Health Effects Institute, 2019).

385

386 While China's pollution is expected to decline in most socio-economic projections, India's is  
387 expected to grow except under strong emissions controls (Samset et al., 2019). Regardless of the  
388 realism of these scenarios, the results should be seen as further impetus for regional policies to  
389 reduce SO<sub>2</sub> emissions given that we have found combined emissions reductions from China and  
390 India can increase monsoon precipitation over the country by 5% on average and by up to 20%  
391 locally. This effect, in combination with consequent impacts of continued growth in GHGs (Figure  
392 S1), could result in an overabundance. This calls therefore for careful consideration of implications  
393 for both precipitation and health over multiple timescales.

394

### 395 **Code and data availability**

396 All code and model data to make the figures used in this paper will be made publicly available  
397 through Zenodo following acceptance of the paper. The ESRL database makes gridded  
398 precipitation data publicly available for both the University of Delaware data



399 ([https://www.esrl.noaa.gov/psd/data/gridded/data.UDel\\_AirT\\_Precip.html](https://www.esrl.noaa.gov/psd/data/gridded/data.UDel_AirT_Precip.html)) and for the GPC  
400 data (<https://www.esrl.noaa.gov/psd/data/gridded/data.gpc.html>).

401

#### 402 **Author contribution**

403 ATA, NLA, JFL, DS, GF ran the RAEI experiments for their respective GCMs. PS prepared the  
404 manuscript with contributions from all co-authors.

405

#### 406 **Competing interests**

407 The authors declare that they have no conflict of interest.

408

#### 409 **Acknowledgments**

410 This study was supported by the Harvard Global Institute. ATA and NLA thank NERC through  
411 NCAS for funding for the ACSIS project and NE/P016383/1. The UKESM work used Monsoon2,  
412 a collaborative High Performance Computing facility funded by the Met Office and the Natural  
413 Environment Research Council. This work used JASMIN, the UK collaborative data analysis  
414 facility. The NCAR-CESM work is supported by the National Science Foundation and the Office  
415 of Science (BER) of the U.S. Department of Energy. NCAR is sponsored by the National Science  
416 Foundation. Climate modeling at GISS is supported by the NASA Modeling, Analysis and  
417 Prediction program. GISS simulations used resources provided by the NASA High-End  
418 Computing (HEC) Program through the NASA Center for Climate Simulation (NCCS) at Goddard  
419 Space Flight Center.

420

#### 421 **References**



- 422 Annamalai, H. and Liu, P., 2005: Response of the Asian Summer Monsoon to changes in El Niño  
423 properties. *Quart. J. Roy. Meteor. Soc.*, **131**, 805-831.
- 424 Annamalai, H., Hamilton, K. and Sperber, K.R., 2007: South Asian summer monsoon and its  
425 relationship with ENSO in the IPCC AR4 simulations. *J. Clim.*, **20**, 1071-1083.
- 426 Bentsen, M., et al., 2013: The Norwegian Earth System Model, NorESM1-M – Part 1: Description  
427 and basic evaluation of the physical climate. *Geosci. Model Dev.*, **6**, 687-720.
- 428 Bollasina, M.A., Ming, Y. and Ramaswamy, V., 2011: Anthropogenic aerosols and the weakening  
429 of the South Asian Summer Monsoon. *Science*, 6055(**334**), 502-505.
- 430 Bond, T.C., et al., 2013: Bounding the role of black carbon in the climate system: A scientific  
431 assessment. *J. Geophys. Res.-Atmos.*, **118**, 5380-5552.
- 432 Chadwick, R., Good, P., and Willett, K.M., 2016: A simple moisture advection model of specific  
433 humidity change over land in response to SST warming. *J. Clim.*, **29**, 7613–7632.
- 434 Conley, A.J., et al., 2018: Multimodel surface temperature responses to removal of US sulfur  
435 dioxide emissions. *J. Geophys. Res.-Atmos.*, **123**, 2773-2796.
- 436 Douglas, E.M., Beltrán-Przekurat, A., Niyogi, D., Pielke, R.A. and Vörösmarty, C.J., 2009: The  
437 impact of agricultural intensification and irrigation on land–atmosphere interactions and  
438 Indian monsoon precipitation – a mesoscale modeling perspective. *Glob. Planet.  
439 Change*, **67**, 117-128.
- 440 Dufresne, J.-L., et al., 2013: Climate change projections using the IPSL-CM5 Earth System Model:  
441 from CMIP3 to CMIP5. *Clim. Dyn.*, 10(**40**), 2123-2165.
- 442 Eyring, V., Bony, S., Meehl, G.A., Senior, C.A., Stevens, B., Stouffer, R.J. and Taylor, K.E., 2016:  
443 Overview of the Coupled Model Intercomparison Project Phase 6 (CMIP6) experimental  
444 design and organization. *Geosci. Model Dev.*, **9**, 1937-1958.



- 445 Health Effects Institute, 2019: State of Global Air 2019. Data source: Global Burden of Disease  
446 Study 2017. *IHME*, 2018.
- 447 Hewitt, H.T., et al., 2011: Design and implementation of the infrastructure of HadGEM3: the next-  
448 generation Met Office climate modelling system. *Geosci. Model Dev.*, **4**, 223-253.
- 449 Kim, M.-K., Lau, W.K.M., Kim, K.-M. and Lee, W.-S., 2007: A GCM study of effects of radiative  
450 forcing of sulfate aerosol on large scale circulation and rainfall in East Asia during boreal  
451 spring. *Geophys. Res. Lett.*, **34**, L24701.
- 452 Koch, D. and Del Genio, A.D., 2010: Black carbon semi-direct effects on cloud cover: review and  
453 synthesis. *Atmos. Chem. Phys.*, **10**, 7685-7696.
- 454 Koch, D., et al., 2009: Evaluation of black carbon estimations in global aerosol models. *Atmos.*  
455 *Chem. Phys.*, **9**, 9001-9026.
- 456 Kumar, K.K., Kumar, R.K., Ashrit, R.G., Deshpande, N.R. and Hansen J.W., 2004: Climate  
457 impacts on Indian agriculture. *International J. of Clim.*, **24**, 1375-1393.
- 458 Liu, L., et al., 2018: A PDRMIP multimodel study on the impacts of regional aerosol forcings on  
459 global and regional precipitation. *J. of Clim.*, **31**, 4429-4447.
- 460 Meehl, G.A., Arblaster, J.M. and Collins, W.D., 2008: Effects of black carbon aerosols on the  
461 Indian Monsoon. *J. Clim.*, **21**, 2869-2882.
- 462 Monerie, P.-A., Robson, J., Dong, B., Hodson, D. L. R., & Klingaman, N. P. (2019). Effect of the  
463 Atlantic multidecadal variability on the global monsoon. *Geophys. Res. Lett.*, **46**, 1765–  
464 1775.
- 465 Neale, R.B., et al., 2012: Description of the NCAR Community Atmosphere Model (CAM 5.0).  
466 NCAR Tech. Note TN-486, 274 pp.



- 467 Paul, S. et al., 2016: Weakening of Indian summer monsoon rainfall due to changes in land use  
468 land cover. *Sci. Rep.*, **6**, 32177.
- 469 Prell, W.L., and Kutzbach, J.E., 1992: Sensitivity of the Indian monsoon to forcing parameters and  
470 implications for its evolution, *Nat.*, **360**, 647–652.
- 471 Priya, P., Krishnan, R., Mujumdar, M., and Houze Jr., R.A., 2017: Changing monsoon and  
472 midlatitude circulation interactions over the Western Himalayas and possible links to  
473 occurrences of extreme precipitation. *Clim. Dyn.*, **49**, 2351-2364.
- 474 Ramanathan, V. and Crutzen, P., 2003: New directions: Atmospheric brown “clouds”. *Atmos.*  
475 *Env.*, **37**, 4033-4035.
- 476 Ramanathan, V., et al., 2005: Atmospheric brown clouds: Impacts on South Asian climate and  
477 hydrological cycle. *PNAS*, 102(**15**), 5326-5333.
- 478 Ramesh, K.V. and Goswami, P., 2014: Assessing reliability of climate projections: the case of  
479 Indian monsoon. *Sci. Rep.*, **4**, 161-174.
- 480 Rao, S., et al., 2017: Future air pollution in the Shared Socio-economic Pathways, *Global Environ.*  
481 *Chang.*, **42**, 346-358.
- 482 Saha, A. and Ghosh, S., 2019: Can the weakening of Indian Monsoon be attributed to  
483 anthropogenic aerosols? *Environ. Res. Commun.*, **1**, 061006.
- 484 Samset, B.H. and Myhre, G., 2015: Climate response to externally mixed black carbon as a  
485 function of altitude. *J. Geophys. Res.*, **120**, 2913-2927.
- 486 Samset, B.H., et al., 2016: Fast and slow precipitation responses to individual climate forcers: A  
487 PDRMIP multimodel study. *Geophys. Res. Lett.*, **43**, 2782-2691.
- 488 Samset, B.H., Lund, M.T., Bollasina, M., Myhre, G. and Wilcox, L., 2019: Emerging Asian  
489 aerosol patterns. *Nat. Geosci.*, **12**, 582-584.



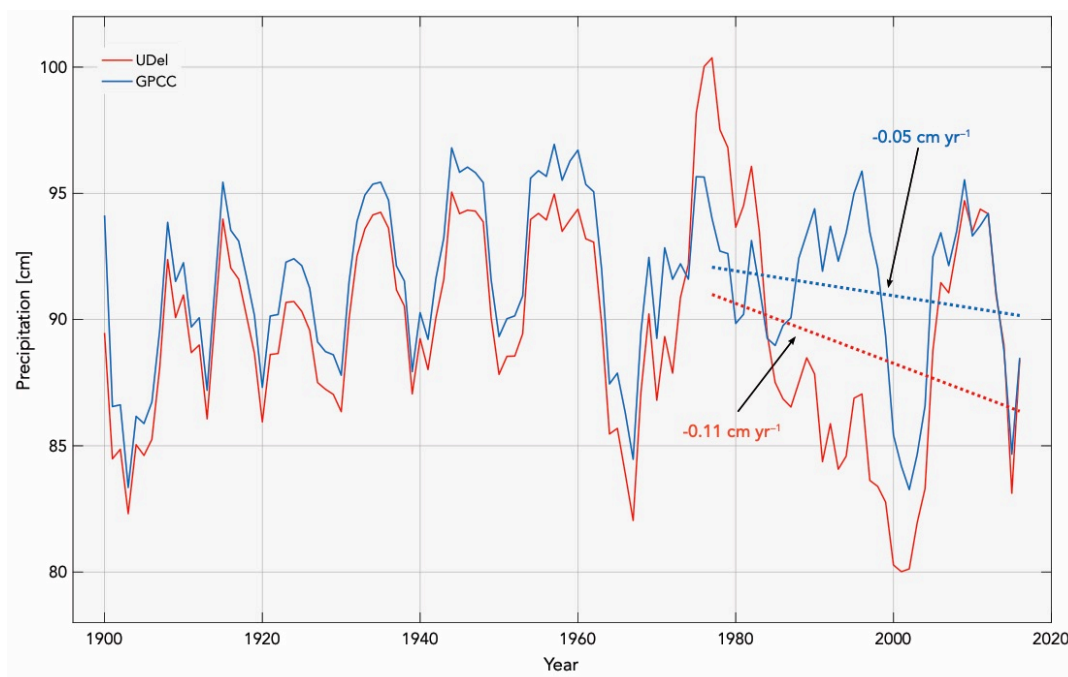
- 490 Schmidt, G.A., et al., 2014: Configuration and assessment of the GISS ModelE2 contributions to  
491 the CMIP5 archive. *J. Adv. Model. Earth Syst.*, **1(6)**, 141-184.
- 492 Schneider, U., Becker, A., Finger, P., Meyer-Christoffer, A. and Ziese, M., 2018: GPCP Full Data  
493 Monthly Product Version 2018 at 0.5°: Monthly Land-Surface Precipitation from Rain-  
494 Gauges built on GTS-based and Historical Data. DOI:  
495 10.5676/DWD\_GPCP/FD\_M\_V2018\_050
- 496 Sellar, A.A., et al., 2019: UKESM1: Description and evaluation of the UK Earth System Model.  
497 *J. Adv. Model. Earth Syst.*, **11**.
- 498 Shawki, D., Voulgarakis, A., Chakraborty, A., Kasoar, M., and Srinivasan, J., 2018: The South  
499 Asian Monsoon response to remote aerosols: global and regional mechanisms. *J. Geophys.*  
500 *Res.*, **123**, 11,585-11,601.
- 501 Shukla, J. and Paolino, D.A., 1983: The Southern Oscillation and long-range forecasting of the  
502 summer monsoon rainfall over India. *Mon. Wea. Rev.*, **111**, 1830-1837.
- 503 Sillmann, J., et al., 2019: Extreme wet and dry conditions affected differently by greenhouse gases  
504 and aerosols. *npj Clim. Atmos. Sci.*, **2**, 24.
- 505 Sikka, D.R., 1980: Some aspects of the large-scale fluctuations of summer monsoon rainfall over  
506 India in relation to fluctuations in the planetary and regional scale circulation  
507 parameters. *Proc. Indian Natl. Acad. Sci.*, **89**, 179-195.
- 508 Stjern, C.W., et al. 2017: Rapid adjustments cause weak surface temperature response to increased  
509 black carbon concentrations. *J. Geophys. Res.*, **122**, 11,462-11,481.
- 510 Subbiah, A. *Initial Report on the Indian Monsoon Drought of 2002* (Asian Disaster Preparedness  
511 Center, 2002).



- 512 Turner, A.G. and Annamalai, H., 2012: Climate change and the South Asian Summer Monsoon.  
513 *Nat. Clim. Change*, **2**, 1-9.
- 514 Wang, C., Kim, D., Ekman, A.M.L., Barth, M.C., Rasch, P.J., 2009: Impact of anthropogenic  
515 aerosols on Indian summer monsoon. *Geophys. Res. Lett.*, **36**, L21704.
- 516 Watanabe, S., et al., 2011: MIROC-ESM 2010: Model description and basic results of CMIP5-  
517 20c3m experiments. *Geosci. Model Dev.*, **4**, 845-872.
- 518 Westervelt, D.M., et al., 2018: Connecting regional aerosol emissions reductions to local and  
519 remote precipitation responses. *Atmos. Chem. Phys.*, **18**, 12461-12475.
- 520 Wilcox, L.J., Highwood, E.J., Booth, B.B.B. and Carslaw, K.S., 2015: Quantifying sources of  
521 inter-model diversity in the cloud albedo effect. *Geophys. Res. Lett.*, **42(5)**, 1568-1575.
- 522 Willmott, C.J. and Matsuura, K., 2001: Terrestrial Air Temperature and Precipitation: Monthly  
523 and Annual Time Series (1950 - 1999),  
524 [http://climate.geog.udel.edu/~climate/html\\_pages/README\\_ghcn\\_ts2.html](http://climate.geog.udel.edu/~climate/html_pages/README_ghcn_ts2.html).
- 525 Xie, X., et al., 2020: Distinct responses of Asian summer monsoon to black carbon aerosols and  
526 greenhouse gases. *Atmos. Chem. Phys. Discuss.*, in review.
- 527



## 528 Figures

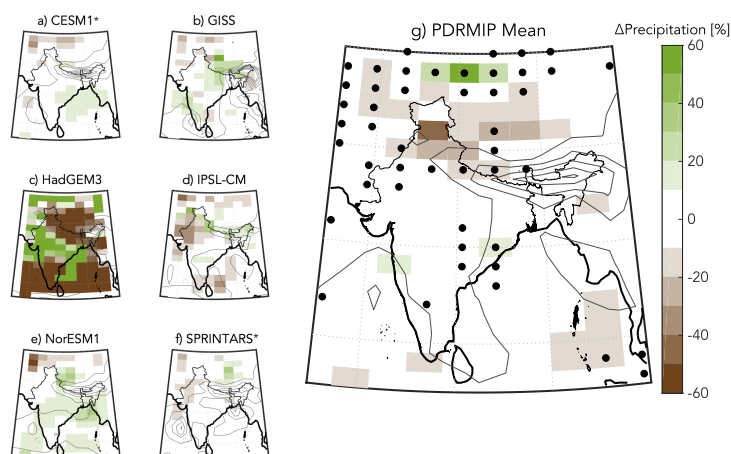


529

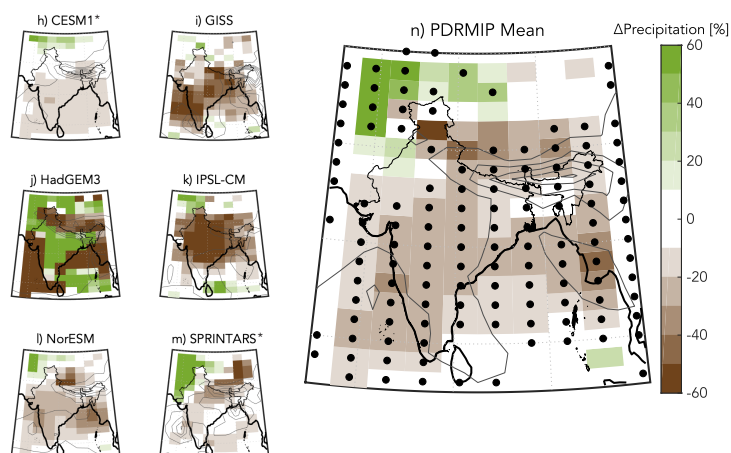
530 **Figure 1.** Average cumulative summer (JJAS) precipitation [cm] over land in all of India from  
531 1900 to 2016 for two observational datasets: (red) University of Delaware (UDeI; Willmot and  
532 Matsuura, 2001) (blue) the Global Precipitation Climatology Center (GPCC; Schneider et al.  
533 2018). Data are smoothed using a moving mean with a window size of five years. Linear trend  
534 lines are indicated for the last 40 years for each dataset as dashed lines, and the slopes [cm yr<sup>-1</sup>]  
535 are denoted by the arrows.



### BC10xASIA – CTRL<sub>PDRMIP</sub>

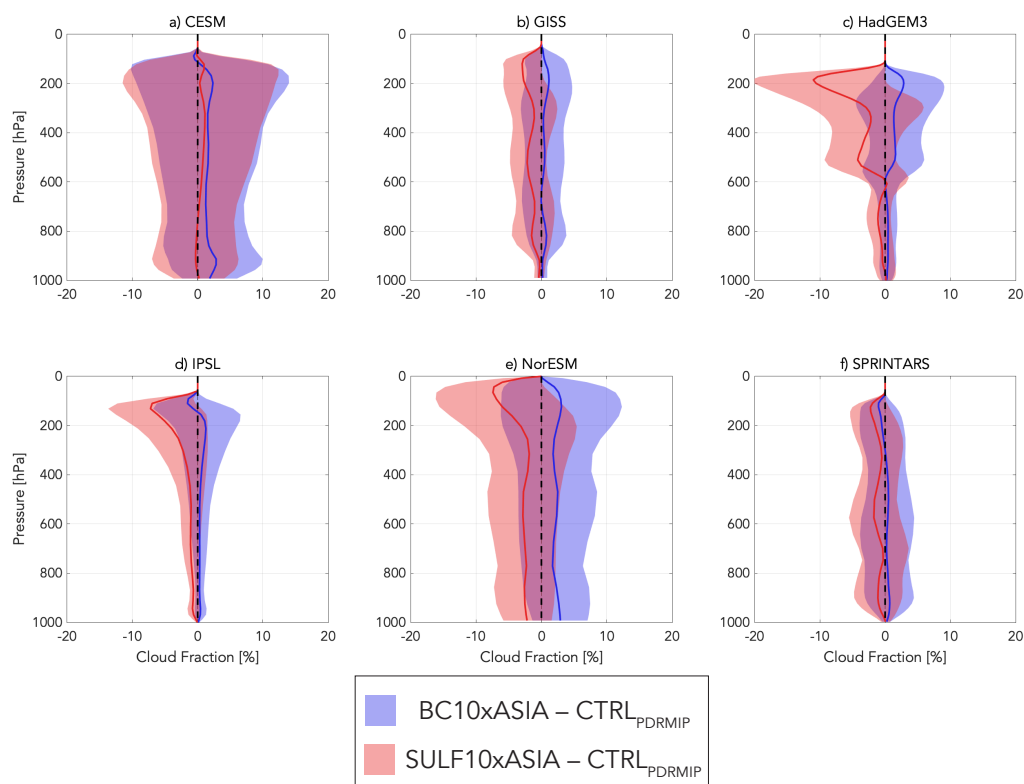


### SULF10xASIA – CTRL<sub>PDRMIP</sub>



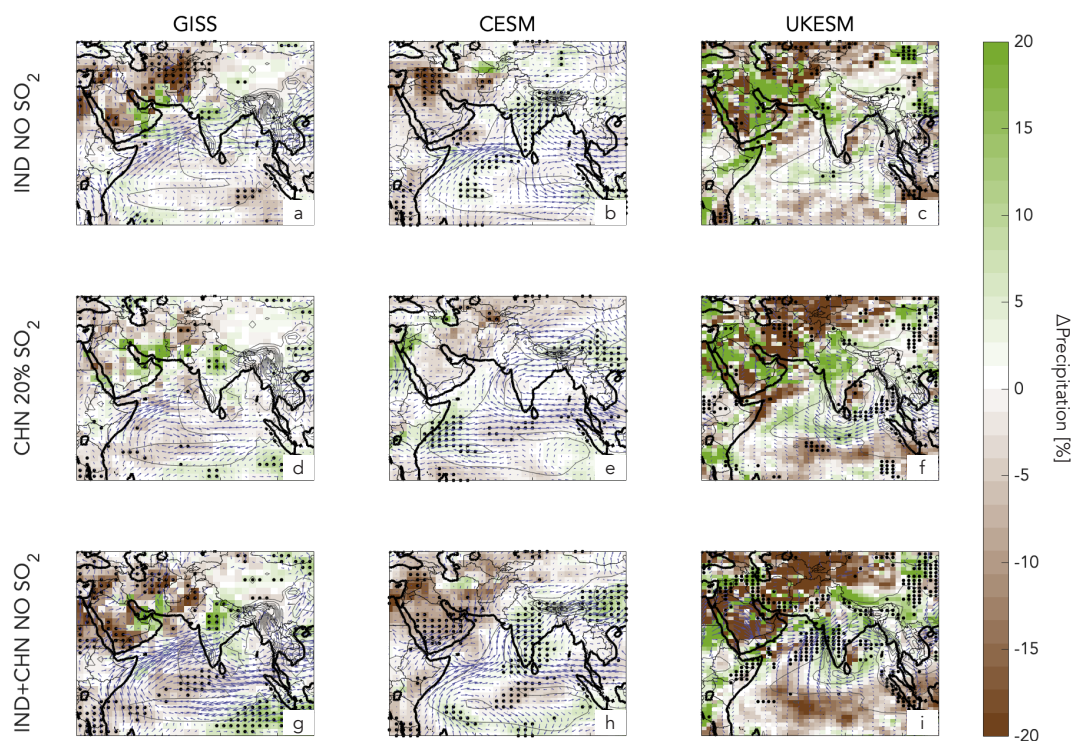
536

537 **Figure 2.** Percent change in summertime (JJAS) precipitation between (a-f) the BC10xASIA and  
538 the CTRL<sub>PDRMIP</sub> runs; (g) the multimodel mean of the change. Similarly, (h-m) represent the  
539 precipitation change in JJAS precipitation between the SULF10xASIA scenarios and the  
540 CTRL<sub>PDRMIP</sub> runs, and (n) represents the multimodel mean of the change. Stippled grid cells in  
541 (g) and (n) denote regions where at least five of the six models agree on the sign of the change.  
542 Grey contours indicate mean JJAS precipitation from the control experiment for each model at 5  
543 mm day<sup>-1</sup> intervals.



544

545 **Figure 3.** JJAS difference in cloud fraction between (blue) the BC10xASIA and the CTRL<sub>PDRMIP</sub>  
546 runs and (red) the SULF10xASIA scenarios and the CTRL<sub>PDRMIP</sub> runs. The bold lines represent  
547 the mean difference and the shadings represent 25<sup>th</sup> and 75<sup>th</sup> percentiles.  
548

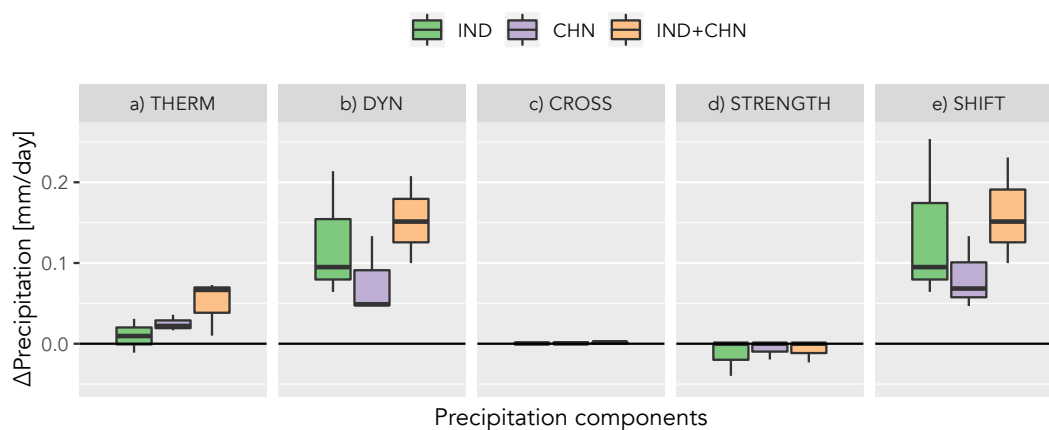


549  
550  
551  
552  
553  
554  
555  
556

**Figure 4.** JJAS precipitation percentage difference between the SO<sub>2</sub> regional emissions scenarios and the CTRL runs. JJAS 850 hPa wind changes are overlaid for each simulation. The columns represent the different models and rows represent the different emissions scenarios. Stippled regions denote areas where the difference is significant at a 90% confidence level for a two-sample t-test. Grey contours indicate mean JJAS precipitation from the control experiment for each model at 5 mm day<sup>-1</sup> intervals.



557



558

559 **Figure 5.** Boxplots indicating the decomposition of area averaged JJAS precipitation anomalies  
560 [mm day<sup>-1</sup>] into a)  $\Delta P_{\text{therm}}$ , b)  $\Delta P_{\text{dyn}}$ , c)  $\Delta P_{\text{cross}}$ , d)  $\Delta P_{\text{strength}}$  and e)  $\Delta P_{\text{shift}}$  components over India.  
561 Different colors represent the three RAEI scenarios relative to the respective CTRL run with  
562 green representing the IND NO SO<sub>2</sub> experiment, purple the CHN 20% SO<sub>2</sub> experiment and  
563 orange the IND+CHN NO SO<sub>2</sub> experiment. The range for each boxplot corresponds to  
564 intermodel variability from the three different models studied in the RAEI experiments.